Chinese Chemical Letters 34 (2023) 107806

Contents lists available at ScienceDirect

Chinese Chemical Letters

journal homepage: www.elsevier.com/locate/cclet

Chemical protein synthesis elucidates key modulation mechanism of the tyrosine-*O*-sulfation in inducing strengthened inhibitory activity of hirudin

Ye Yang[a], Mingchan Liang[b], Rui Wang[b,*], Chunmao He[a,*]

[a] School of Chemistry and Chemical Engineering, South China University of Technology, Guangzhou 510640, China
[b] Pingshan translational medicine center, Shenzhen Bay Laboratory, Shenzhen 518118, China

ARTICLE INFO

Article history:
Received 11 July 2022
Revised 30 August 2022
Accepted 2 September 2022
Available online 6 September 2022

Keywords:
Tyrosine sulfation
Hirudin
Chemical protein synthesis
Post-translational modification
Native chemical ligation

ABSTRACT

Tyrosine sulfation is an important post-translational modification that enhances the inhibitory activity of hirudin. Herein, we developed a facile synthetic strategy to afford the sulfated hirudins with up to three modifications and in multi-milligram scales, after a single HPLC purification step. Through these synthetic proteins, a novel type of modulation mechanism exhibited by tyrosine sulfation was proposed, which would help to delineate the structure–function relationships in other sulfated proteins and more importantly, to serve as a basis for the development of related antithrombotic agents.

Thrombin is a central enzyme in the blood coagulation pathway where it cleaves the fibrinogen into insoluble fibrin [1]. Hirudin, originated from the salivary gland of the leech *Hirudo medicinalis*, is among the most potent natural inhibitors of thrombin [2], which inspired the development of a number of antithrombotic agents for clinic applications [3]. Crystallographic studies have established the critical role of the rather compact N-terminal region of hirudin in the direct blockade of the active site of thrombin [4–6]. The rather disordered C-terminal tail binds in an extended conformation on the surface of the hirudin, which contains a high number of basic residues—also known as the anion-binding exosite I or the fibrinogen recognition exosite (Fig. 1A) [7]. While electrostatic interactions between the many acidic residues in the C-terminal of hirudin and exosite I play a critical role in establishing the tight and specific hirudin–thrombin binding, thereby competing with its native substrate fibrinogen, extensive mutagenesis studies have unraveled a number of important hydrophobic interactions in this region, involving Phe56 and Tyr63 (Fig. 1B) [8]. Importantly, the tyrosine *O*-sulfation—a wide-spread post-translational modification found in most natural hirudin variants, has been shown to be critical for the high inhibitory activity [2]. As shown in X-ray crystal structure (Fig. 1D), the additional salt bridge formed between the sulfate group of Tyr63 of hirudin variant-1 (HIRV1) and Lys81 in the exosite I of the thrombin was believed to be the key factor [9]. On the contrary, mutation of Tyr63 to Phe only lead to minimum change in the inhibitory activity of HIRV1 [8], indicating that other molecular mechanisms besides the electrostatic interactions may contribute to the strengthened inhibitory activity upon sulfation.

Interestingly, the rather conserved Phe56 of HIRV1 is located in a hydrophobic binding pocket composed of Met32, Phe34, Leu40, Arg67 and Arg73 from thrombin (Fig. 1B), and is able to mediate the tight binding and hence the inhibition of hirudin towards thrombin [8,10,11]. A direct comparison of the X-ray crystal structures of the thrombin complex with the non-sulfated and sulfated HIRV1 reveals a local structural rearrangement upon sulfation at Tyr63, which moves Phe56 further into the hydrophobic binding pocket (Figs. 1C and D). However, quantitative data on the impact of sulfation toward the structural changes at Phe56 and its inhibitory activity are currently not available. In order to address this issue, the sulfated HIRV1 was chemically synthesized by the native chemical ligation (NCL) method and the photo-active *p*-benzoylphenylalanine (Bpa) was incorporated at position 56, and the corresponding structural changes and inhibitory activities were investigated.

Initially, the peptide bond between Asn38–Cys39 was selected as the ligation site, with the aim of shortening the peptide fragment that contains the modification sites, *i.e.*, HIRV1(39–65), as much as possible [12–14]. However, attempted synthesis of the N-terminal peptide thioester fragment HIRV1(1–38) *via*

* Corresponding authors.
E-mail addresses: wangrui@szbl.ac.cn (R. Wang), hecm@scut.edu.cn (C. He).

https://doi.org/10.1016/j.cclet.2022.107806
1001-8417/

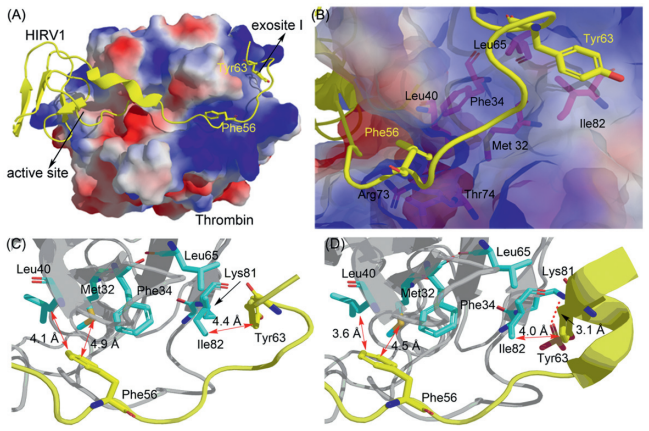

Fig. 1. Cyrstallographic structures of the hirudin–thrombin complex. Schematic representations of the overall structure (A) and major exosite I interactions (B) of the hirudin–thrombin complex (PDB code 4HTC), thrombin is shown by its electrostatic surface potential and hirudin as a yellow ribbon. Comparison of the major hydrophobic interactions in the thrombin complex with the non-sulfated (PDB code 4HTC) (C) or sulfated (PDB code 2PW8) (D) hirudin. The red double-headed arrows denote key inter-residue distances and the dashed line denotes the salt bridge. All figures were generated with PyMOL.

solution-phase thioesterifation [15] only resulted in minor product as followed by RP-HPLC analysis (Data not shown). Instead of trying to improve the synthetic yield of the peptide thioester fragment HIRV1(1–38), we switched to a different synthetic route where Lys27–Cys28 was chosen as the ligation site (Fig. 2A). In the new disconnection strategy, although the peptide fragment with the modification sites is longer, the N-terminal peptide thioester fragment HIRVI(1–27) can now be synthesized *via* the peptide hydrazide method [16,17]. As such, peptide hydrazide **1** was obtained *via* standard Fmoc-SPPS, and was conveniently transferred to the corresponding peptide thioester **2** *via* Dawson's acetyl acetone (acac)-activation method [18]. The neopentyl (nP) protection group for sulfate of the tyrosine was reported to be stable against routine Fmoc-SPPS and TFA cleavage conditions [19], hence Fmoc-Tyr(SO_3nP)-OH was chosen as the monomer for the installation of the sulfo-tyrosine. The C-terminal peptide fragments **3**–**6** with up to three sidechain modifications were obtained in 4.3%–4.9% yield (Figs. S6–S9 in Supporting information). Notably, besides the sulfated Tyr63 and Bpa56, biotin was attached to the sidechain of Lys47 in peptides **5** and **6** to assist the purification or enrichment if needed.

With all the required peptides in hand, we firstly tested the ligation between peptides **2** and **3** in a typical NCL buffer (6 mol/L Gdn·HCl, 0.2 mol/L Na_2HPO_4, pH 6.5). Noted that there are four Cys-residues in the peptide thioester **2**, and an internal thiolactone **2′** was formed immediately when **2** was dissolved in the NCL buffer (Fig. S4 in Supporting information). Nevertheless, when 0.67 equiv. of **3** was added, the ligation with **2′** went smoothly to afford the full-length protein **7**, albeit a bit slower (*i.e.*, completed within 24 h). Next, the ligation product **7** was purified by HPLC before it was subjected to oxidative refolding. While the refolding process was essentially completed in 5 h, the total synthetic yield over the two steps was lower than 10% (Fig. S11 in Supporting information). In an effort to improve the overall yield, we explored the ligation and refolding without intermediate HPLC purification [20,21]. For this purpose, the ligation mixture was exchanged into a buffer containing 6 mol/L Gnd-HCl, 0.2 mmol/L PBS, pH 6 by ultracentrifugation (3 kDa cut-off) and was directly added drop-wise into the refolding buffer (final conc. 0.2–0.4 mg/mL). The refolding was typically completed within 5–16 h, and the resulting mixture was purified by HPLC to afford the native HIRV1 **11** in a yield of

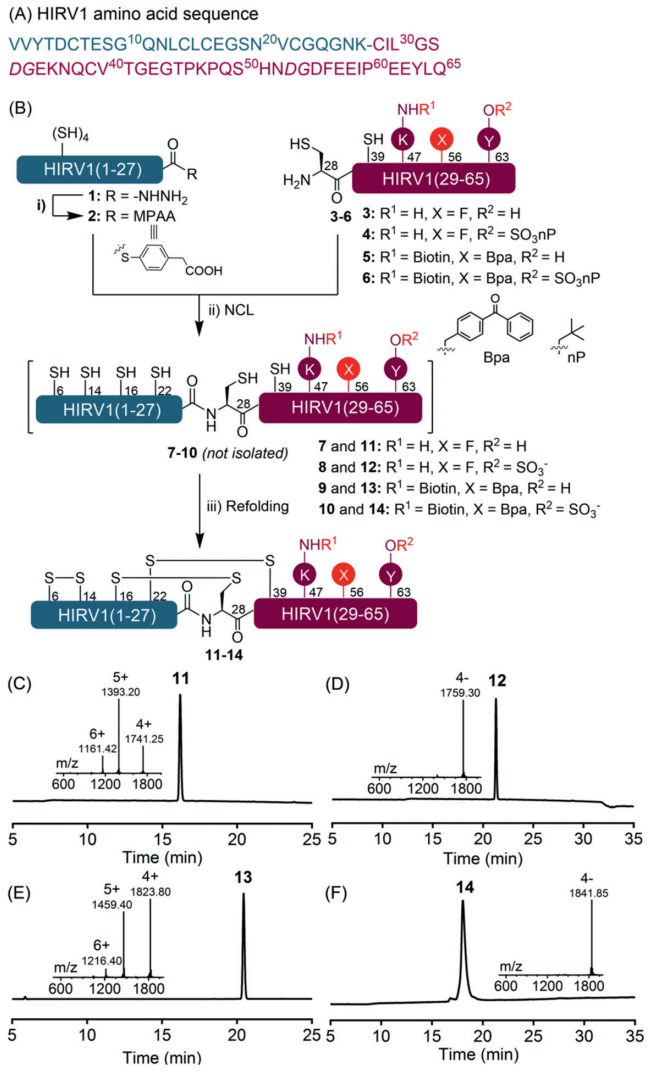

Fig. 2. Total chemical synthesis of the HIRV1 variants. (A) The amino acid sequence of native HIRV1. (B) Scheme for the facile synthesis of the HIRV1 variants **11**–**14**. Reaction conditions: i) 6 mol/L Gdn·HCl, 0.2 mol/L Na_2HPO_4, 10 equiv. MPAA, 2.5 equiv. acac, pH 3.0, 25 °C, 10 h; ii) 6 mol/L Gdn·HCl, 0.2 mol/L Na_2HPO_4, 200 mmol/L MPAA, 40 mmol/L TCEP, pH 6.5, 25 °C, 4–12 h; iii) 0.2 mol/L Tris, 4 mmol/L L-cysteine, 2 mmol/L L-cystine, 4 mol/L NaCl, pH 8.5, 25 °C, 5–16 h. (C–F) Analytical HPLC (214 nm) and ESI-MS characterization of the folded HIRV1 variants **11**–**14**. **12** and **14** were measured in the negative mode to obtain the mass spectrum of the labile sulfate group.

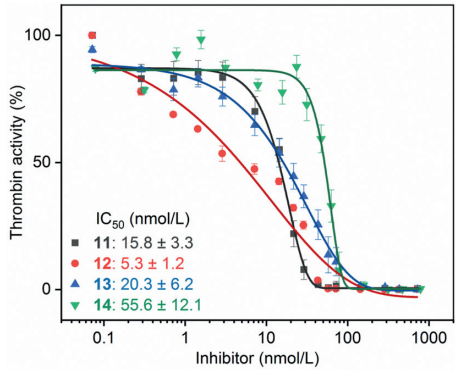

Fig. 3. Inhibition of the fibrinogenolytic activity of bovine thrombin by the synthetic HIRV1 variants **11** to **14**. IC_{50} values were calculated using a sigmoidal dose-response function, and are shown as mean ± standard deviation of at least three independent experiments.

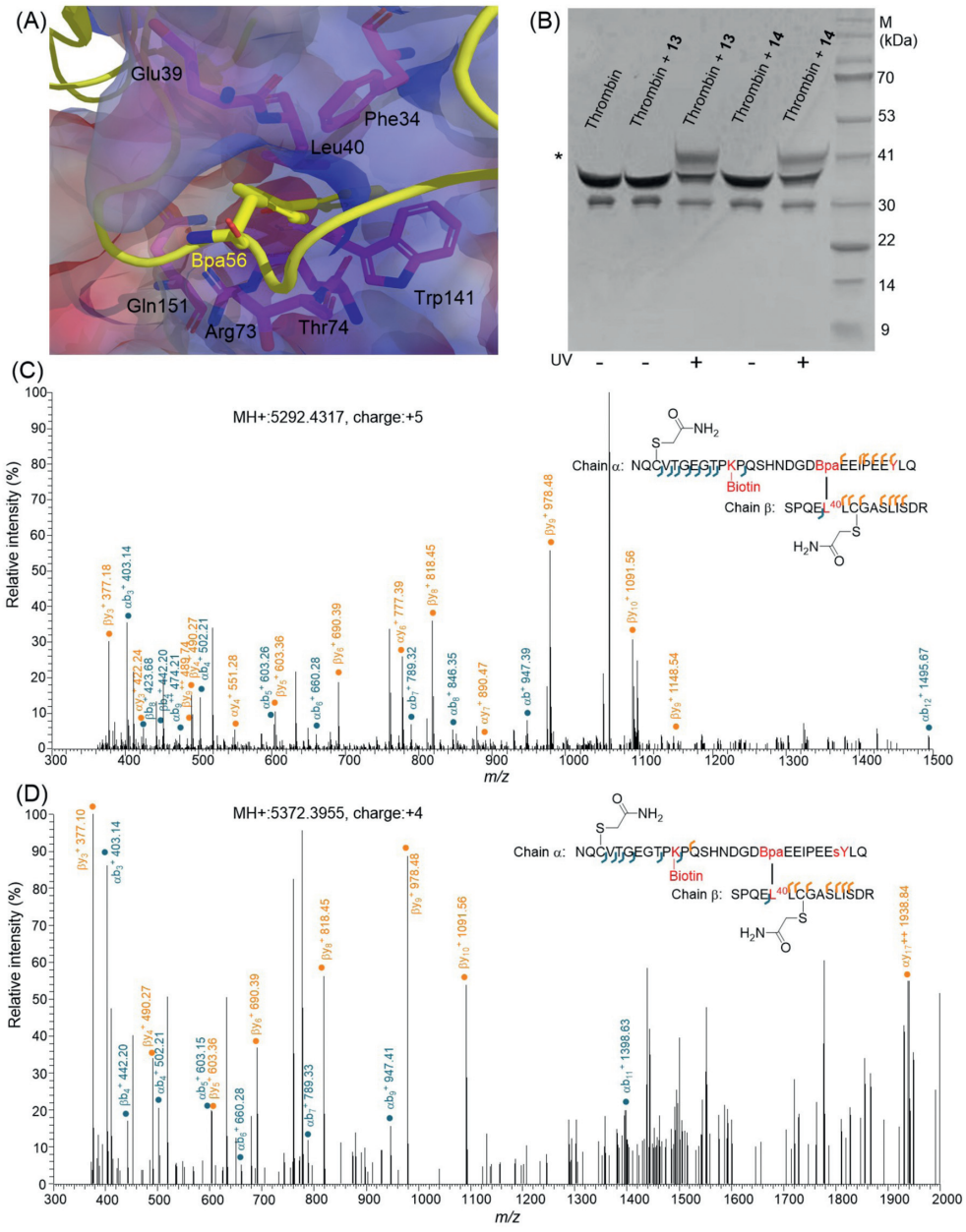

Fig. 4. Investigation of the interacting residues of Bpa56 in the hydrophobic binding pocket by photo-crosslinking. (A) Key residues surrounding Bpa56 inside the binding pocket as modeled and visualized with PyMOL. (B) SDS-PAGE analysis of the photo-crosslinking process. Note the lower band above 30 kDa is from the original thrombin sample, possibly the heavy chain (see Supporting information); * indicates the conjugated product band. (C, D) MS/MS analysis of the digested photo-crosslinked product of peptide fragments between thrombin with **13** (C) and **14** (D). sY indicates the sulfation at Tyr63.

19%. With this optimized strategy, the other three HIRVI variants **12**, **13** and **14**, were obtained with yields between 20%–30% after a single HPLC purification step, and in multi-milligram scales (Figs. 2B–F). It is worth mentioning that the nP protection group was removed automatically during the ligation processes, as was also observed by us and other groups previously [22,23]. Finally, the correct disulfide pairing mode was confirmed by thermolysin/trypsin digestion and HPLC-MS analysis (Figs. S21–S24 in Supporting information), which set the stage for biological studies.

With all the desired modifications installed on the synthetic HIRV1 variants, we firstly investigated their effect on the inhibition of the fibrinogenolytic activity of bovine thrombin. For this purpose, bovine thrombin (5 U/mL) was incubated with HIRV1 variants **11**–**14** at varied concentrations for ~1 h prior to the addition of fibrinogen (7 μmol/L). The optical turbidity at 405 nm was followed to afford the inhibition of the fibrinogenolytic activity (IC_{50}) of thrombin. In agreement with the literature [2], sulfation at Tyr63 indeed strongly strengthened HIRV1's inhibitory activity, as judged from the IC_{50} values, *i.e.*, $IC_{50} = 15.8$ nmol/L for the native HIRV1 **11** *vs.* $IC_{50} = 5.3$ nmol/L for **12** (Fig. 3). Interestingly, incorporation of biotin to the sidechain of Lys47 and replacement of Phe56 with Bpa into the non-sulfated HIRV1 seems to have a negligible influence on its inhibitory activity, as indicated from the similar IC_{50} values observed between the native HIRV1 **11** and **13**. These modifications, however, exhibit a notable impact on the inhibitory activity of the sulfated proteins, with a tenfold increase of the IC_{50} value in **14** compared to **12**. As the Lys47 residue would be too far away from the exosite I to affect the interaction between HIRV1 and thrombin, Phe56 was proposed to be the key influencing residue. It suggests that the sulfation of Tyr63 could lead to

a minor structural rearrangement in the C-terminal tail such that the Phe56 residue fit better and further inside into its hydrophobic binding pocket. This is achieved through mostly hydrophobic interactions as highlighted in the X-ray crystal structure, with additional contribution from the salt bridge between the Tyr63(SO_3^-) of HIRV1 and Lys 81 of thrombin (Fig. 1D). As such, stronger inhibitory activity was observed in the sulfated HIRV1 variant **12** in comparison to the native HIRV1 **11**; if Phe56 was replaced with the more steric demanding Bpa, a tight fit into the binding pocket would be less likely and hence resulted in the much weakened inhibitory activity of **14**.

To further probe whether the sulfation of Tyr63 could affect the interacting residues of Phe56 inside the binding pocket, a photo crosslinking strategy was adopted. As mentioned, Phe56 was replaced by Bpa in two of the synthetic HIRV1 variants, *i.e.*, **13** and **14**, which upon exposure to UV irradiation can be covalently crosslinked to its interacting residues (Fig. 4A) [24–26]. The two HIRV1 variants were incubated with thrombin for 1–2 h at 37 °C to establish a complete binding, and afterwards, UV irradiation was applied and the crosslinking process was followed by SDS-PAGE analysis. As shown in Fig. 4B, a new band appeared only in the photo-irradiated samples. The band was then sliced and destained, further followed in-gel tryptic digestion [27]. The digested peptides were extracted, desalted and subjected to liquid chromatography tandem mass spectrometry (LC–MS/MS) analysis to directly collect data. The data were analyzed with pLink v2.3.11 and the matched mass spectral peaks of cross-linked fragments were exported with pLabel v2.4.1 [28–30]. Noted that a biotin sidechain was also incorporated at the Lys47 in both variants to assist the peptide enrichment, but it was found to be unnecessary in the final established protocol. As shown in Fig. 4C, a mass peak (5292.4317 Da) corresponding to the fragmentation precursor mass $[M+5H]^{5+}$ of crosslinked peptides between thrombin and **13** was found, to allow the unambiguous identification of the conjugation site at thrombin to be Leu40. Similarly, the fragmentation precursor mass $[M(SO_3^-)+5H]^{4+}$ of crosslinked peptides between thrombin and **14** also elucidated Leu40 as the conjugation site (Fig. 4D). Altogether, we concluded that while the sulfation at Tyr63 leads to a better fit of Phe56 into the binding pocket, it would not affect the interacting residue.

In summary, we have established a robust synthetic strategy to afford the sulfated HIRV1 with up to three modifications and in multi-milligram scales. With the help of the photo-active Bpa we were able to elucidate the molecular mechanism of sulfation at Tyr63 in enhancing the inhibitory activity of HIRV1, and a tight fit of Phe56 in the hydrophobic binding pocket of thrombin upon Tyr63 sulfation was proposed. Together with the direct electrostatic interaction, they represent, to our knowledge, a novel type of modulation mechanism exhibited by tyrosine sulfation, which would help to delineate the structure–function relationships in other sulfated proteins and more importantly, to serve as a basis for the development of related antithrombotic agents.

Declaration of competing interest

The authors declare the following financial interests/personal relationships which may be considered as potential competing interests:

A Chinese patent is filed covering the synthetic strategy for sulfated hirudins described in this manuscript (Application No. 202210261766.X).

Acknowledgments

The financial support from the National Natural Science Foundation of China (Nos. 91853117 and 22077036); the Natural Science Foundation of Guangdong Province (No. 2020A1515010766) are greatly acknowledged.

Supplementary materials

Supplementary material associated with this article can be found, in the online version, at doi:10.1016/j.cclet.2022.107806.

References

[1] F. Markwardt, Semin. Thromb. Hemost. 28 (2002) 405–414.
[2] S.R. Stone, J. Hofsteenge, Biochemistry 25 (1986) 4622–4628.
[3] M.Á. Corral-Rodríguez, S. Macedo-Ribeiro, P.J. Barbosa Pereira, et al., J. Med. Chem. 53 (2010) 3847–3861.
[4] T.J. Rydel, A. Tulinsky, W. Bode, et al., J. Mol. Biol. 221 (1991) 583–601.
[5] T.J. Rydel, K.G. Ravichandran, A. Tulinsky, et al., Science 249 (1990) 277–280.
[6] M.G. Grütter, J.P. Priestle, J. Rahuel, et al., EMBO J. 9 (1990) 2361–2365.
[7] J.W. Fenton, Semin. Thromb. Hemost. 15 (1989) 265–268.
[8] A. Betz, J. Hofsteenge, S.R. Stone, Biochemistry 30 (1991) 9848–9853.
[9] C.C. Liu, E. Brustad, W. Liu, et al., J. Am. Chem. Soc. 129 (2007) 10648–10649.
[10] G. Cristalli, P. Franchetti, M. Grifantini, et al., J. Med. Chem. 30 (1987) 1686–1688.
[11] S.J.T. Mao, M.T. Yates, T.J. Owen, et al., Biochemistry 27 (1988) 8170–8173.
[12] Y.S.Y. Hsieh, L.C. Wijeyewickrema, B.L. Wilkinson, et al., Angew. Chem. Int. Ed. 126 (2014) 4028–4032.
[13] R. Mousa, T. Hidmi, S. Pomyalov, et al., Comm. Chem. 4 (2021) 30.
[14] Z. Zhao, R. Mousa, N. Metanis, Chem. Eur. J. 28 (2022) e202200279.
[15] S. Flemer Jr, J. Pept. Sci. 15 (2009) 693–696.
[16] G. Fang, Y. Li, F. Shen, et al., Angew. Chem. Int. Ed. 50 (2011) 7645–7649.
[17] J. Zheng, S. Tang, Y. Qi, et al., Nat. Protoc. 8 (2013) 2483–2495.
[18] D.T. Flood, J.C.J. Hintzen, M.J. Bird, et al., Angew. Chem. Int. Ed. 57 (2018) 11634–11639.
[19] L.S. Simpson, J.Z. Zhu, T.S. Widlanski, et al., Chem. Biol. 16 (2009) 153–161.
[20] P. Liao, C. He, Front. Chem. 9 (2021) 735149.
[21] P. Liao, H. Liu, C. He, Chem. Sci. 13 (2022) 6322–6327.
[22] R.E. Thompson, X. Liu, J. Ripoll-Rozada, et al., Nat. Chem. 9 (2017) 909–917.
[23] C. Li, C. He, Org. Biomol. Chem. 18 (2020) 7559–7564.
[24] W.F. Herblin, J.C. Kauer, S.W. Tam, Eur. J. Pharmacol. 139 (1987) 273–279.
[25] K.F. Taupitz, W. Dörner, H.D. Mootz, Chem. Eur. J. 23 (2017) 5978–5982.
[26] N. Chu, A.L. Salguero, A.Z. Liu, et al., Cell 174 (2018) 897–907.
[27] M. Huynh, P. Russell, B. Walsh, Methods Mol. Biol. 519 (2009) 507–513.
[28] Z. Chen, J. Meng, Y. Cao, et al., Nat. Commun. 10 (2019) 3404.
[29] D. Li, Y. Fu, R. Sun, et al., Bioinformatics 21 (2005) 3049–3050.
[30] L. Wang, D. Li, Y. Fu, et al., Rapid Commun. Mass Spectrom. 21 (2007) 2985–2991.